On the Origin of Elements in the Milky Way

Reto Trappitsch

Spring semester 2021

Contents

Contents

Preface

These lecture notes for the course "On the origin of the elements in the Milky Way" are prepared as we go, so they will be in part influenced by you! If you find typos, errors, or other issues please let me know. The most recent copy of the LaTeX files and figures can also be found on GitHub.

The lecture notes contain clickable links, e.g., all references are linked to the bibliography and all acronyms are linked to the acronyms' definition page. These links are generally colored in dark blue.

The end of the document contains a bibliography that contains details on all references. Note that references here are limited and often point to review articles that could be of interest to the reader. More detailed references to individual topics can be found in these articles. Each reference entry contains a digital object identifier (doi)[1] that can be found online and accessed via a Brandeis library subscription. Alternatively, a link to ArXiV[2] is provided.

Specific boxes throughout the text discuss further information. They are defined as following:

Background information on topics that do not necessarily fit into the text but are important to keep in mind will be given in a box like this.

Further information and reading for the avid reader will be pointed out in a box like this. The scope of these boxes is generally slightly outside the realm of the class.

Programming is an integral part of scientific research, be it for running experiments, performing measurements, evaluating measurements, or modeling a system. A box like this will point you to more information with respect to coding. These boxes will often refer to coding in python.

---

[1] https://doi.org
[2] https://arxiv.org

Acronyms

r-**process** rapid neutron capture process

s-**process** slow neutron capture process

AU astronomical unit

BBN Big Bang nucleosynthesis

CMB cosmic microwave background

dex decimal exponent

doi digital object identifier

EUV extreme ultraviolet

GCE galactic chemical evolution

HST Hubble Space Telescope

IMF initial mass function

IR infrared radiation

ISM interstellar medium

MESA Modules for Experiments in Stellar Astrophysics

pc parsec

pdf portable document format

SN supernova

SOHO solar and heliospheric observatory

UV ultraviolet

WMAP Wilkinson microwave anisotropy probe

1. Solar System Abundances

To understand the origin of the elements in the Milky Way, it is crucial to first understand what in fact needs explaining. One of the best studied points in the history of the Milky Way is the Solar System we inhabit, mainly since we actually live inside it and thus have direct access to its material.

The Solar System formed $4.567\,\mathrm{Ga}$ ago from a homogeneous molecular cloud. Since the Milky Way itself formed roughly $13\,\mathrm{Ga}$ ago, the molecular cloud from which the solar nebula formed evolved for roughly $8.4\,\mathrm{Ga}$ since the formation of the Milky Way and around $9\,\mathrm{Ga}$ since the Big Bang. The process that describes the formation and destruction of elements over this period of time is generally referred to as galactic chemical evolution (GCE).

In order to put the Solar System abundances in perspective to the galaxy, Figure 1.1 shows a schematic of the Milky Way (left). The galactic center, which is likely a black hole, is surrounded by an area called the bulge. The disk of the Milky Way has a spiral structure. An analogue galaxy with a similar structure is UGC 12158, shown on the right in Figure 1.1. The densest regions of the Milky Way are close to the center (e.g., the bulge) while less dense areas are further out (e.g., the disk). The Solar System is located in the disk and about two-thirds out from the center in one of the spiral arms called the Orion-Cygnus arm. Disk and bulge are both surrounded by a low-density halo. This halo also contains globular clusters, which are gravitationally bound aggregations of stars. These clusters tend to be very old and are thus made of material that formed early on in the history of the Milky Way.

This chapter discusses the composition of the Solar System $4.567\,\mathrm{Ga}$ ago (the initial Solar System abundances) and today (abundances in the solar photosphere). While we can observe stars and determine their composition via spectroscopy, the Solar System is unique since we have meteorites available that represent unaltered solar nebula material. This material is especially useful since it can be studied in the laboratory using mass spectrometry techniques.

Initial Solar System abundances in python can easily be handled with the `iniabu` package. This package can be used make various databases of Solar System abundances available for interaction and is used here to create abundance plots using `matplotlib`. Full disclosure: I am the author of the package and am thus surely biased.
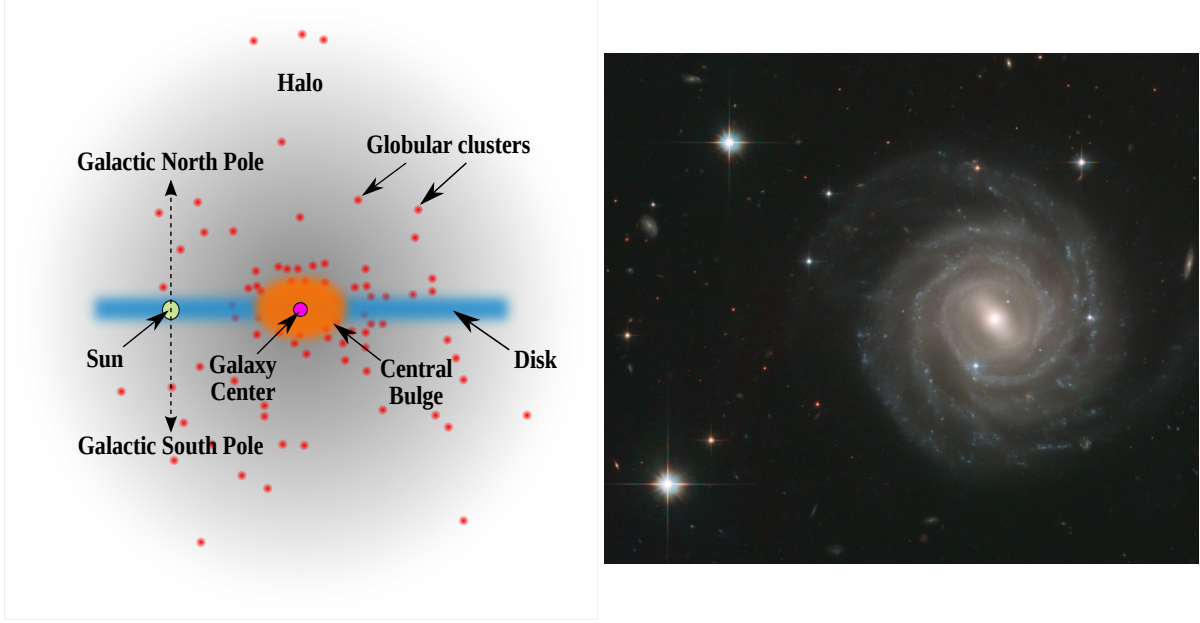
Figure 1.1.: *Left: Profile of the Milky Way with the current position of the Solar System indicated. Edited from Wikipedia. Right: Galaxy UGC 12158, which is thought to have a similar spiral structure as the Milky Way. Credit: ESA/Hubble & NASA*

1.1. Definitions and Notations

1.1.1. Terminology

Elemental concentrations and abundances are two terms that are often used interchangeably and their meaning, unfortunately, is often ambiguous. Let us for example look at a form of uranium oxide named yellowcake. The chemical formula for a common form of yellowcake is U_3O_8, i.e., the smallest unit consists of three uranium atoms and eight oxygen atoms. Expressing the stoichiometric elemental abundance of oxygen in yellowcake, i.e., the abundance by number of atoms, we would say that the oxygen abundance of yellowcake is $8/(8+3) = 0.73$. Alternatively and often (but not exclusively referred to as the concentration) we could determine the oxygen concentration by mass. Uranium (mean mass: $\bar{m}_U = 237.3\,u$) is significantly heavier than oxygen (mean mass: $\bar{m}_O = 16.0\,u$). The mean mass here is the mass averaged over all isotopes of the specific element. The average concentration of oxygen in yellowcake, by mass, can then be determined as:

$$[O] = \frac{8\bar{m}_O}{8\bar{m}_O + 3\bar{m}_O} = 0.15 \tag{1.1}$$

Note that when solar abundances with respect to meteorites, the stoichiometric / number abundances are generally used. Astronomers and astrophysicists on the other hand often

report mass fractions (see below).

Solar (elemental) mass fractions are commonly used in astronomy. For astronomers, the universe consists, to first order, of three elements, namely hydrogen (X), helium (Y), and metals (Z), which are all elements heavier than helium. This might sound strange since it implies that the air we breathe (78% nitrogen, 21% oxygen) consists of metals in the astronomical sense, however makes some sense when looking, e.g., at the composition of the Sun. The Sun's composition in this notation is $X = 0.7389$, $Y = 0.2463$, and $Z = 0.0148$. These mass fractions are always given by weight.

Solar System initial abundances, often referred to as Solar System abundances, describe the original composition of the Solar System 4.567 Ga ago. To determine this composition, measurements of, e.g., meteorites must be decay corrected for radioactive nuclides and their products.

Solar photospheric abundances on the other hand refer to the present-day composition of the Sun. There are further important differences between initial and present-day abundances that are discussed in the subsequent sections.

> **Radioactive decay** Unstable atomic nuclei undergo radioactive decay to so-called daughter nuclei. For example, ^{26}Al is an unstable isotope and decays to the stable ^{26}Mg. Its half-life ($t_{1/2}$), which is the time after which only half the initial material is left, is 7.17×10^5 a. Radioactive decay is an exponential process. Instead of the half-life the decay constant $\lambda = \ln 2 / t_{1/2}$ is often referred to. Radioactive decay can be calculated as:
>
> $$N(t) = N_0 \exp\left(-\lambda t\right) \tag{1.2}$$
>
> Here, N_0 is the amount of radioactive material available at $t = 0$ and $N(t)$ is the amount of material after time t has elapsed.

1.1.2. Scales

As with definitions, several different scales are used. Here we define the three most commonly used ones. **Meteoritic abundances** are generally normalized to the number of silicon atoms, which is set to be equal to $N_{\mathrm{Si}} = 10^6$. These abundances scale linearly.

Spectroscopic abundances, often used in astronomy, are frequently given with respect to hydrogen, the most abundant element in the universe. These abundances are usually reported as logarithmic abundances and the abundance of hydrogen is defined to be equal to 12. For example, the Solar System initial abundance of silicon in this logarithmic unit can be calculated as:

$$A(\mathrm{Si}) = \log_{10}\left(\frac{N_{\mathrm{Si}}}{N_{\mathrm{H}}}\right) + 12 = 7.59 \tag{1.3}$$

Here, N_{Si} and N_{H} are the number abundances of silicon and hydrogen, respectively.

Finally, **mass fractions** are also frequently used in astronomy and astrophysics. The mass fraction of an element or isotope x_i with number abundance N_i and mass m_i can be calculated as:

$$x_i = \frac{N_i m_i}{\sum_j N_j m_j} \tag{1.4}$$

Here, the sum over j adds up all elements or isotopes. If we were thus to sum up all mass fractions, we would get $\sum_j x_j = 1$.

1.1.3. Comparing measurements

In astronomy, chemical abundance ratios are generally expressed in "bracket"-notation. These chemical abundance ratios are then usually regarded with respect to a standard, which generally is the Sun. For example, to express the iron content of a given star in comparison to the Sun one would calculate:

$$[\text{Fe/H}] = \log_{10}\left(\frac{N_{\text{Fe}}}{N_{\text{H}}}\right)_{\text{star}} - \log_{10}\left(\frac{N_{\text{Fe}}}{N_{\text{H}}}\right)_{\odot} \tag{1.5}$$

Here, N_x represents the number abundance of a given element x. The symbol $\odot$ is generally used for the Sun. Using this formulation, observations with higher iron content than the Sun would result in a positive number, and vice verse. While the [Fe/H] number is unitless, differences in this notation are commonly referred to as decimal exponent (dex). A star with a $0.3\,\text{dex}$ enhancement in [Fe/H] would thus have twice as much iron than the Sun when normalized to hydrogen.

1.2. The Sun

The Sun is the central body of the Solar System and contains with a mass of $\sim 2 \times 10^{30}\,\text{kg}$ about 99.86% of the total mass in the Solar System. The total luminosity of the Sun is $3.8 \times 10^{26}\,\text{W}$ and it's orbited by the Earth at a mean distance of $\sim 1.5 \times 10^{8}\,\text{km}$, which is equal to 1 astronomical unit (AU). The total solar irradiance at Earth is thus around $1.3\,\text{kW/m}^2$.

Since the Sun contains the majority of the Solar System's mass, it is reasonable to assume that this celestial body also represents well the Solar System's composition. Figure 1.2 shows an artistic rendering of the structure of the Sun. The Sun's core extends to about a quarter of its radius and is the main nuclear engine that fuses hydrogen to helium at a temperature of around $16 \times 10^6\,\text{K}$.[1] The solar core is not convectively connected to the outer layers, thus energy is mainly transported by radiative transfer.

---

[1] Temperatures in astrophysics are often written as $T_x = y$. In this case, the actual temperature would be $y \times 10^x\,\text{K}$. For the core of the Sun we could write the temperature thus as $T_{10} = 1.6$.
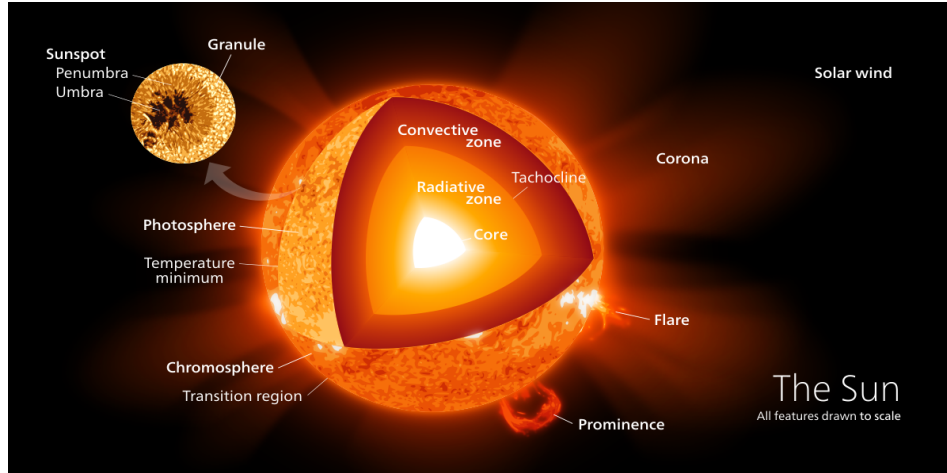
Figure 1.2.: *The structure of the Sun. Credit:* Wikipedia

The photosphere, which is the visible part of the Sun, is at a temperature of around 5800 K. The atmosphere of the Sun has a minimum temperature of around 4100 K about 500 km above the photosphere. It consists of the chromosphere which lays above the photosphere and the solar corona that extends from the chromosphere out into space. At higher altitudes the temperature of the corona increases and reaches temperatures in excess of 10^6 K. How such high temperatures can be reached in the solar corona is still unclear.

Wien's displacement law states that the radiation curve of a black-body has it's peak at different wavelengths depending on the temperature. For a given temperature, the peak wavelength can be calculated as:

$$\lambda_{\mathrm{max}} = \frac{b}{T} \tag{1.6}$$

Here, T is the temperature in kelvin and $b = 2.898 \times 10^{-3}$ m·K. Plugging in the photosphere temperature, we can calculate a peak wavelength at 500 nm, which is the color green in the visible part of the electromagnetic spectrum.

1.2.1. Spectroscopy and Absorption Spectra

In order to determine the composition of the Sun from the electromagnetic spectrum it radiates, astronomers use a technique called stellar spectroscopy. Using a prism or grating the light from the Sun is dispersed into its individual colors. Figure 1.3 shows the electromagnetic spectrum of the Sun between 380 nm and 710 nm. Clearly visible are dark spectral absorption lines, so-called Fraunhofer lines named after Joseph von
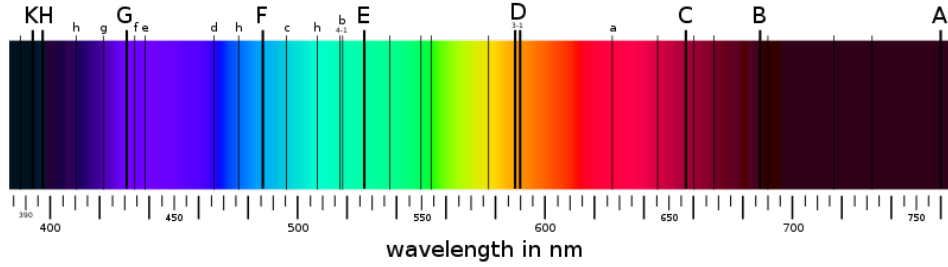
Figure 1.3.: *The solar spectrum broken up into its components. Credit:* Wikipedia.

Fraunhofer who discovered, studied, and described them in 1814.

These absorption lines are fingerprints of the Sun's elemental composition. The dark lines form since photons coming out of the Sun are absorbed in the photosphere by atoms. The absorbed photons are subsequently re-emitted, however, this re-emission is not directed. Thus, the area of the spectrum that the original photon was absorbed in appears darker. For example, the double lines labeled "D" in Figure 1.3 are a feature of the sodium absorption lines.

1.2.2. Stellar Abundances

In order to interpret the Fraunhofer lines observed from the Sun with respect to its elemental composition, many physical parameters and models must be known. Here we give a brief overview of these modeling efforts. Further details can be found in two great reviews on determining the Sun's elemental composition by Asplund et al. (2009) and Allende Prieto (2016).

To determine the composition of the Sun two closely related conditions must be understood: (1) line formation and (2) the stellar atmosphere. These two fields include physics from several disciplines, namely fluid dynamics, statistical mechanics, and thermodynamics. To understand line formation the atomic parameters and stellar conditions, such as the opacity, need to be known. To model stellar atmospheres on the other hand we need to know the energy radiated through the atmosphere, the surface gravity, and the chemical composition. Note that the chemical composition is on one hand what we would like to determine from these observations, however it is also an integral part of the stellar atmospheric model. The chemical composition has thus to be determined in an iterative process. For a given set of interest, especially the amount of energy radiated through it, its surface gravity, and its chemical composition. Note that the chemical composition, which is what we would like to find, must be known in order to model the stellar atmosphere. Determining the composition of the Sun from observations is thus an iterative process. For a given model atmosphere and determined atomic and molecular lines and continuum opacities, so-called spectra synthesis codes can be used

to predict the spectrum of the model star with all its absorption lines. These spectra are then compared to observations. If different, the parameters, especially the chemical composition is updated with better values and the models are run again. The chemical composition of the star is found when model and observations agree.

Photospheric Abundances

The solar photosphere (see Figure 1.2) is the part of the Sun that we can actually see. Spectroscopy of the photosphere is thus generally used to model the solar abundances. With a temperature between 4500 K and 6000 K and an effective temperature of around 5800 K no molecules can form in the photosphere and thus only atoms are expected to contribute to its absorption lines. Furthermore, the densities of the chromosphere and corona above the photosphere are so low that they do not influence the absorption lines observed from the photosphere.

   The present-day solar photosphere composition is slightly different from the initial Solar System abundance, i.e., the abundance that is representative of the homogeneous solar nebula. One difference of course is for radioactive nuclides that have decayed over the last 4.567 Ga since the beginning of the Solar System. Furthermore, thermal diffusion, gravitational settling, and radiative acceleration – the three of which are often collectively referred to as diffusion – also changed the photospheric composition over the past 4.567 Ga. Corrections for these effects must thus be applied before comparing Solar System initial abundances, as e.g., measured in meteorites (see Section 1.3) with photospheric measurements.

Chromosphere & Corona Observations

The chromosphere and corona are the solar layers right above the photosphere. These layers are too thin for us to directly observe and can generally only be seen during a total solar eclipse. Since there is no homogeneous background irradiation for the chromosphere and corona in these cases, absorption spectra cannot be measured. Thus, the elemental composition of the solar atmosphere is determined by measuring emission spectra. Excited atoms fall back to their ground states at discreet energies. Such emission lines will show up as bright instead of dark lines when analyzed in a spectrograph.

   Temperatures as low as 4100K have been measured in the chromosphere. This allows for the existence of simple molecules, which complicates the determination of the spectral abundances since many more atomic transitions are suddenly available. Furthermore, the chromosphere has a fairly large temperature gradient which also complicates the models.

   Coronal abundances are difficult to determine. The extremely high temperatures of the coronal make it difficult to determine radiative transitions in the laboratory. A large part of the coronal emission lines are furthermore in the ultraviolet (UV) and extreme
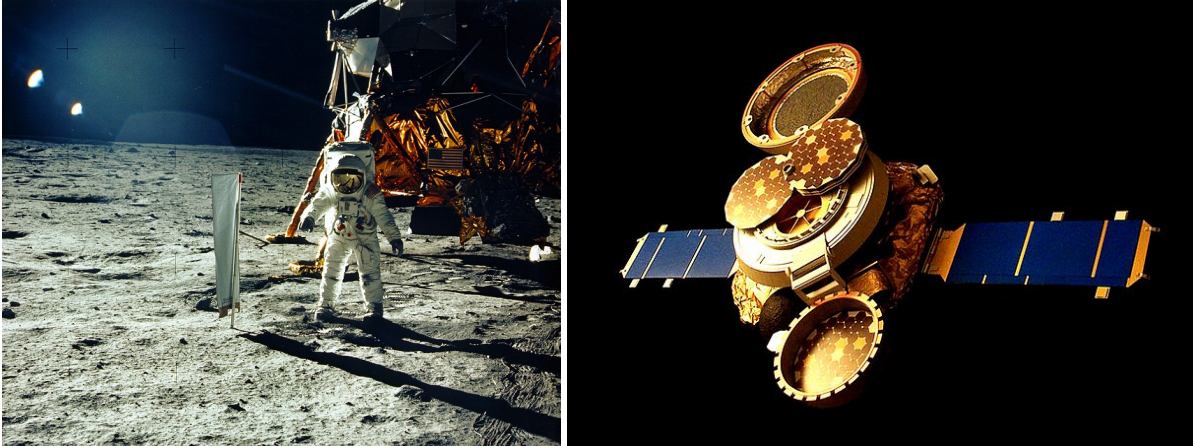
(a) *Buzz Aldrin standing next to the solar* **(b)** *Artist conception of the Genesis spacecraft* *sail during the Apollo 11 mission.* *with unfolded collectors.*

Figure 1.4.: *The two types of solar wind catcher experiments that have been used to determine the composition of the Sun. Credit: NASA*

ultraviolet (EUV), thus can not be detected from Earth due to the atmosphere. Spacecrafts such as solar and heliospheric observatory (SOHO) have been used to determine the elemental composition of the solar corona.

Solar Wind

Mass ejections such as prominences and flares (see Figure 1.2) are the origin of the solar wind that penetrates the whole Solar System. The interaction of the solar wind with the Earth's magnetic field can, e.g., be seen as aurorae (borealis and australis), also known as the northern and southern lights. The solar wind consists to 98% of protons (charged hydrogen particles). The other 2% is mainly charged helium nuclei and a minute amount of heavier particles. This however means that the solar wind does carry some part of the Sun's composition out through the solar system.

While the solar wind cannot be measured on Earth, bodies without an atmosphere such as the Moon are constantly struck by solar wind. During the Apollo missions to the Moon, astronauts carried a solar sail, which was aluminum foil mounted on a pole in order to capture solar wind during their stay on the Moon. Figure 1.4a shows Apollo 11 astronaut Buzz Aldrin standing next to the solar sail. While valuable measurements were done using solar sails flown on Apollo missions, the total exposure time of the aluminum foil was very limited, i.e., only up to a few days each. Thus, only little material was captured which resulted in significant analytical uncertainties when measuring the captured content.

In 2001, NASA launched the Genesis spacecraft which was parked on a Lagrange

point L_1.[2] L_1 is a gravitationally semi-stable place in space in between the Sun and the Earth. Genesis exposed its collectors (Figure 1.4b) to the solar wind for a total of 850 d before returning to Earth. In order to avoid any contamination with terrestrial material, NASA's plan was for Genesis to re-enter the Earth's atmosphere, deploy its drogue parachute, and then capture the capsule mid-air using a helicopter with a long hook. The deployment mechanism for the parachute was connected to an accelerometer, which was unfortunately built backwards into the spacecraft. This resulted in the accelerometer measuring the acceleration with the wrong sign, thus never triggering the software to release the parachute. Needless to say that the "landing" of Genesis took place at a terminal velocity of around $86 \, \mathrm{m \, s^{-1}}$ (190 mph). This broke open the collector container and all collectors were significantly contaminated with material from the Utah dessert. Nevertheless, all main objectives of Genesis could still be achieved by meticulously cleaning and puzzling the collector array back together, a process that took several years.

1.3. Meteorites

Meteorites are rocks that originated in the Solar System and fell to Earth as meteors. They are either finds, meaning that they were found during searches, or falls, meaning that they were found after observing the meteor in the sky. Meteorites could have previously been part of another planet, e.g., Mars, part of the Moon, or, most often, part of an asteroid. Thousands of these rocks have been analyzed, and they are generally classified into various different groups. The two major groups these rocks belong to relate them to their origin; they were either part of a differentiated or an undifferentiated parent body. A differentiated Solar System body has at some point in its history gotten hot enough in order to be completely or partially molten. This separated the metal-loving (siderophile) from the silicate loving (lithophile) elements. The Earth for example is a differentiated body with an iron, nickel core at the center and a silicate mantle around it. Meteorites from undifferentiated bodies, called chondrites, still contain the metal and silicate in the same phases, i.e., they have never gotten hot enough to differentiate.

In order to determine the initial Solar System composition by analyzing meteorites, samples that have never been altered throughout its history are of special interest. These meteorites are called primitive. The most primitive subgroup of the chondrites are the carbonaceous chondrites, which have generally not even been heated enough in order to destroy the mineral phases that originally condensed from the solar nebula.

Alterations different from heat, e.g., chemical alterations, can also influence the composition and thus primitiveness of a meteorite. Meteorites that have been the least altered with respect to their chemical and isotopic composition are carbonaceous chondrites that are similar to the Ivuna meteorite, which is the type specimen for this group.

---

[2]For more information, see https://en.wikipedia.org/wiki/Lagrangian_point

The name of this chondrite group is thus abbreviated CI chondrites. The Orgueil meteorite, a CI chondrite, represents the best studied sample for the Solar System initial abundance. This rock fell on May 14, 1864 just after 8pm local time near Orgueil, a town in southern France. Samples were recovered immediately, totaling 14 kg of material. Meteorite falls have the advantage that they did not spend any significant amounts of time exposed to the weather on Earth, thus they do not show any terrestrial alteration either.

To determine the composition of meteorites, their material is usually homogenized and then analyzed using a mass spectrometery. Depending on the element of interest sample material is atomized and ionized. These ions are then separated by mass-over-charge in a mass analyzer. This allows for precise determination of their elemental and isotopic composition.

Stardust Some primitive meteorites contain micrometer sized grains that in fact did not form in the Solar System at all but rather represent bonafide stardust grains. These stardust grains formed in the outflow of dying stars, were transported through the interstellar medium (ISM), and then incorported into meteorite parent bodies during their formation. We will discuss stardust grains in more detail later since these samples allow us to directly probe the processes in which elements are created.

## 1.4. The Composition of the Solar System

While CI chondrites seem to be primitive Solar System objects, their total mass is represents only a tiny fraction of the total mass of the Solar System. Photosphere observations on the other hand are associated with larger measurement uncertainties and require modeling of the physical processes underlying the formation of absorption spectra. The question thus arises on how the composition of the Solar System can best be determined.

1.4.1. Comparing CI chondrites and the Photosphere

Figure 1.5 shows the comparison of the photosphere measurements reported in Asplund et al. (2009) with the CI chondrite measurements reported in Lodders (2020). Most elements lie perfectly on the 1:1 correlation indicated in black in the figure, which spans a total of around 12 orders of magnitude. However, there are some very notable deviations that require further discussion.

Lithium is the only element that is more abundant in CI chondrites than in the Sun. In the Sun, lithium diffuses effectively. Since it is destroyed during the nuclear reactions
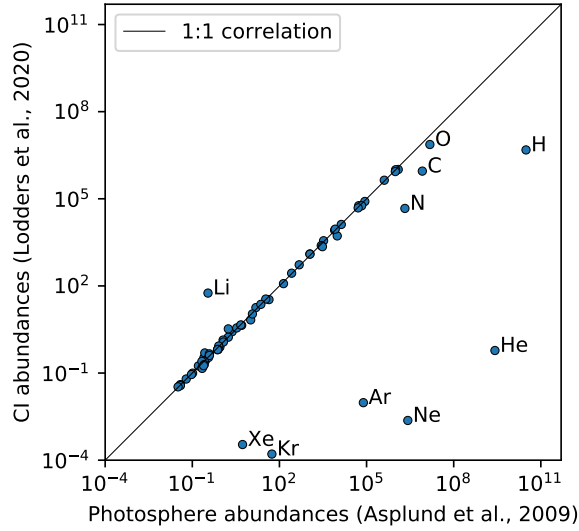
Figure 1.5.: *Comparison of solar photosphere measurements (Asplund et al., 2009) and the composition of CI meteorites (Lodders, 2020). Elements that do not lie close to the 1:1 correlation line are labeled.*

taking place in the stellar core, the overall abundance of lithium is expected to be depleted when compared to the bulk Solar System.

The noble gases helium, neon, argon, krypton, and xenon are all very volatile and are thus heavily depleted in meteorites, i.e., they never effectively condensed into the rocky material when meteorite parent bodies formed. The bulk Solar System helium abundance can fortunately be derived from helioseismology via observations of the Sun and is not highly model dependent. Various techniques have been used to determine the composition of the other noble gases. One of the most accurate methods to-date is the analysis of solar wind in the Genesis collectors, see page 10.

Hydrogen is also a highly volatile element and thus does not effectively condense into meteorite parent bodies. Hydrogen thus needs to be measured in the Sun by model comparison. The hydrogen mass is insensitive to the Z/X composition of the Sun, which results in an accurate determination of the hydrogen mass fraction X.

Carbon, nitrogen, and oxygen are prominent atoms that form volatile molecules, e.g., CO, CO_2, N_2, and O_2. Thus, these elements are expected to be depleted in rocky materials. While these elements can all be measured in the solar photosphere, model improvements resulted in significant changes over time in their abundances.
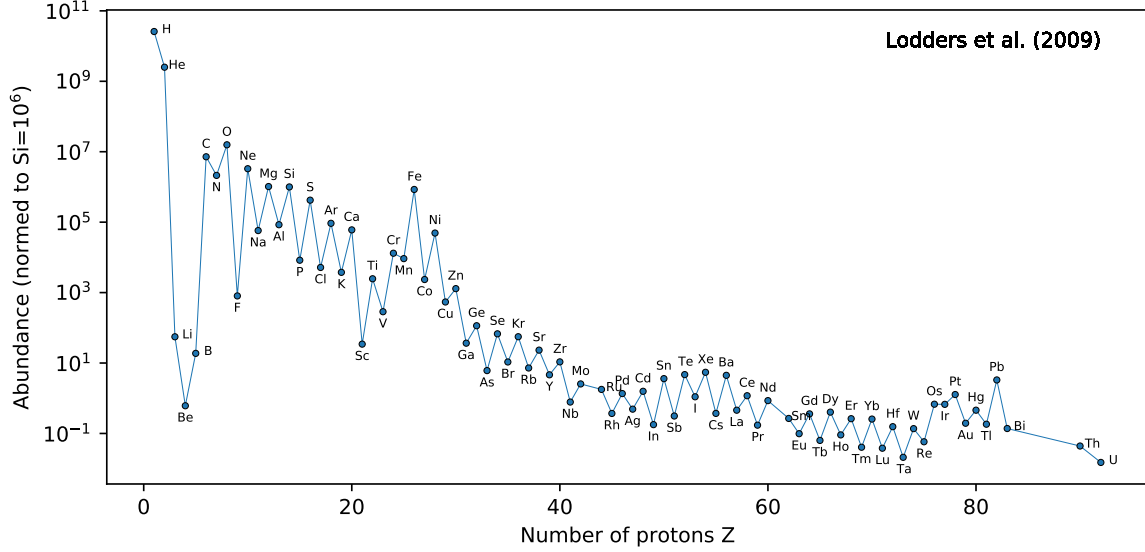
Figure 1.6.: *Solar System initial abundances for all elements (Lodders et al., 2009).*

1.4.2. Solar System Elemental Abundances

Figure 1.6 shows the elemental abundances of the solar nebula. Clearly, hydrogen and helium are the most abundant elements. Furthermore, we can see a clear peak around carbon, oxygen, and neon. These elements are made in most stars and thus reach such high abundances. There is also a clear peak at the iron isotopic composition. This is due to the fact that in this region, the binding energy per nucleon is the highest across all elements. That means that energy can be gained by fusing nuclides together up to iron. Past iron this does not happen anymore, thus the abundances of all heavier nuclides drop significantly.

Another striking feature of the abundance curve in Figure 1.6 is the clear zigzag pattern. This pattern is due to the fact that even nuclei, i.e., nuclei with an even number of nucleons (protons and neutrons), have a higher binding energy than odd nuclei and are thus more stable.

1.4.3. Solar System Isotopic Abundances

So far we have mostly discussed the abundance of the elements in the Solar System. Just as important is the abundance of the isotopes, which can be derived from CI chondrites with high precision. Atomic line differences of individual isotopes are generally too small in order to derive useful isotopic abundances from solar observations. Let us briefly discuss the origin of a few important isotopes cannot easily be derived from CI chondrites.

Deuterium and ^{3}He are both highly volatile, thus cannot be measured in CI chondrites, and have been significantly changed in the Sun. In its early stage the Sun underwent deuterium burning, essentially leaving it deuterium free at this point. This burning also produced ^{3}He and thus changed its abundance in the Sun. The exact D/H ratio in the Solar System is still an active matter of research. Good analogues to determine this ratio are the atmosphere of Jupiter which consists mainly of the gaseous material that the solar nebula was made of, and in comets. Certain, so-called Kuiper-belt comets formed far out in the Solar System beyond the snow-line, which is the area of the solar nebula beyond which water only appears in solid form. These comets thus trapped the original D/H composition. For the early Solar System ^{3}He/^{4}He ratio, the value for Jupiter's atmosphere is generally adopted.

Carbon, nitrogen, and oxygen are all very volatile. While the carbon isotopic composition in the Solar System is not very variable across different types of meteorites, the nitrogen and oxygen isotopic composition vary widely. To measure these isotopes in solar wind was one of the main objectives of the Genesis mission. After significant cleaning of these collectors, the solar oxygen and nitrogen isotopic composition have finally been determined by McKeegan et al. (2011) and Marty et al. (2011), respectively.

Noble gases are also volatile. As discussed before, their elemental and isotopic abundances were determined using the solar wind collectors on board the Genesis spacecraft. A detailed review of this work can be found in Heber et al. (2009).

1.4.4. Preview on the Origin of Elements and Isotopes

So far we have only briefly discussed the major features visible in the Solar System abundance pattern (Figure 1.6). We will look into a lot more details on how individual elements and groups formed later on. The production of elements and their isotopes takes place in a process called nucleosynthesis. A brief overview of these processes is given below.

All hdrogen and helium in universe formed right after the Big Bang in a process called Big Bang nucleosynthesis. The majority of all heavier elements were subsequently formed in stars. Elements up to the iron peak formed mainly in massive stars by nuclear fusion reactions. As discussed before, the binding energy per nucleon is the highest at iron and thus fusion reactions beyond this region are not energetically favorable. Thus, other processes must take over.

Most isotopes beyond iron are formed by neutron-capture reactions. Since neutrons are not electrically charged, they do not see the Coulomb barrier of a positively charged nucleus and can thus be more effectively added to it. Neutron addition takes place until the nucleus becomes unstable. Unstable, neutron-rich nuclei decay generally via

β^--decay to the next stable isobar, which has one proton more and one neutron less. Proton-rich nuclei, e.g., ^{92}Mo, cannot form by neutron capture and various processes and locations for their formation are actively being discussed in the astrophysics community.

About half the elements beyond iron formed in the so called slow neutron capture process (*s*-process), in which the β^- decay to the stable isobar generally happens faster than another neutron can be captured. This way however, only elements up to bismuth can be made. Heavier elements, e.g., actinides such as thorium and uranium, cannot be formed in the *s*-process. Rapid capture of neutrons, the so-called rapid neutron capture process (*r*-process), must thus be invoked to explain their existence.

1.5. Other Stars

While we have Solar System samples, i.e., CI chondrites, to determine the composition of the solar nebula and thus the Sun precisely, representative rocks of other stars are not available in the Solar System. However, the light of other star still reaches us, i.e., we can see their photosphere and apply the same spectroscopic techniques to determine their elemental composition.

As discussed in Section 1.2.2, to determine the abundances of observed other stars, the stellar atmosphere must be modeled. For this, the size and mass of the star must be known, which is not always simple to determine from observations. Recent massive surveys such as the Sloan Digital Sky Survey[3] and the Gaia mission[4] have made it possible to determine the elemental composition of many more stars. An overview of existing database can, e.g., be found in Allende Prieto (2016). It turns out that the solar neighborhood is a diverse place (see, e.g., Bensby et al., 2014) and still leaves us for the time being with many open question on the origin of its elements and isotopes.

1.6. Reading

A great reading to further dive into the topic of solar abundances is the recent review by Lodders (2020).[5] Some questions and points of discussions for this paper are:

- Why are meteoritic measurements normalized to a silicon abundance of 10^6 while astronomical observations are generally given in dex noramlized such that the abundance of hydrogen is equal to 12?

- Why can elemental abundances with much higher precision in CI chondrites than in the Sun's photosphere?

---

[3]https://www.sdss.org/
[4]https://sci.esa.int/web/gaia/
[5]At the time of this writing, the download of the document as a portable document format (pdf) file did not succeed. You can also find this article on ArXiV.

- Why does aqueous alteration not affect the chemical composition of CI chondrites?

- Explain from a nuclear physics point of view why there is no deuterium in the Sun.

- Why is it so difficult to determine certain elemental and isotopic abundances, e.g., noble gases and the D/H ratio of the Solar System?

- What are the difficulties that one encounters when analyzing meteorites by mass spectrometry?

- Why can carbon, oxygen, and nitrogen not be determined when analyzing meteorites?

2. Big Bang Nucleosynthesis

In order to understand primordial / Big Bang nucleosynthesis (BBN), we need to first look at some fundamental observations that define cosmology. In addition, we also need to introduce the standard model of cosmology. Note that this is only a very brief introduction into a topic that could be a whole course by itself.

2.1. Fundamental Cosmological Observations

2.1.1. Olbers' paradox

One of the most fundamental observations that goes back to Kepler (1610), Halley (1721), de Cheseaux (1744), and is today known as Olbers' (1823) paradox is the fact that the night sky is dark. If one assumes an infinite, homogeneous space filled with stars, this space would appear infinitely bright to the observer on Earth. The apparent luminosity of a star can be described as

$$l = \frac{L}{4\pi r^2} \propto r^{-2}, \tag{2.1}$$

where L is the star's luminosity and r its distance from Earth. Assuming a density of stars n, a spherical shell of thickness dr at distance r from Earth would contain

$$dN = 4\pi n r^2 dr \propto r^2 \tag{2.2}$$

stars. The total energy density of all stars for an observer can thus be calculated as

$$\varepsilon_s = \int_0^\infty \frac{L}{4\pi r^2} dN = nL \int_0^\infty dr. \tag{2.3}$$

In contrast to our experience this integral is divergent, thus the night sky should be infinitely bright.

This paradox cannot be simply solved by assuming absorption of light in the interstellar medium, e.g., by dust. The energy from all stars would over time heat up this dust until it radiates as bright as the stars themselves. One factor that slightly helps is that stars will overlap with each other. You can picture this scenario however like standing in a dense forest where, as far as you can see, every line of sites terminates in

a tree trunk. For the universe this would mean that every line of sight will terminate at the surface of a star. Stars cover each other, so the night sky would not seem infinitely bright but homogeneously about as bright as the Sun. This still does not agree with our experience.

The solution to the paradox lies in the fact that the universe is expanding. The wavelength of the light that arrives expands along with the universe and is thus shifted to the red (Doppler shift). The result is that the relative luminosity, as given in equation (2.1), is in fact $l \propto r^{-3}$. Plugging this into equation (2.1) results in the integral converging. In addition, there the universe has a horizon at distance

$$R \simeq ct. \tag{2.4}$$

Here, c is the speed of light and t the approximate age of the universe. The visible part of space and thus the energy density become finite.

Doppler effect Let us assume that a source emits an electromagnetic wave with wavelength λ_s. An observer that moves with a velocity $\vec{v}$ with respect to that source will register a shifted frequency λ_r. For light, and considering special relativity, this effect will result in a blueshift if the observer moves towards the source and in a redshift if the observer moves away from the source. For two objects that move directly towards or away from each other, the relativistic Doppler shift for light can be written as

$$\lambda_r = \sqrt{\frac{1+\beta}{1-\beta}} \lambda_s, \tag{2.5}$$

where $\beta = v/c$, i.e., the speed of the observer v with respect to the speed of light c. Sources moving away from each other hereby have a postive velocity ($\beta > 0$), sources moving towards each other a negative one ($\beta < 0$).

2.1.2. Hubble's Law

The expansion of the universe can in fact be observed. Figure 2.1 shows the Hubble diagram for many observations, taken from Freedman et al. (2001). The diagram on top shows the velocity of objects relative to Earth as a function of their distance. Using the Doppler shift one can see that the velocity, which is away from the observer in this case, is proportional to the redshift of the object. Here, the distance is given in megaparsec, where 1 parsec (pc) is approximately 3.26 light years. The linear relationship between velocity and distance (R) can be written as

$$\left(\frac{\dot{R}}{R}\right)_0 = H_0 = \text{constant.} \tag{2.6}$$
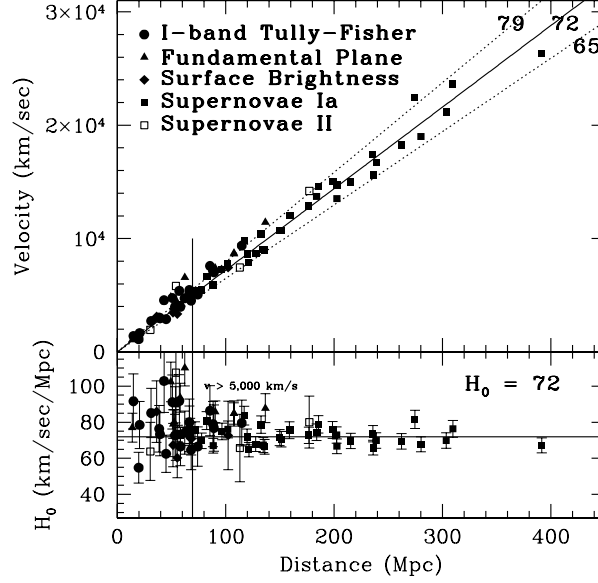
Figure 2.1.: *Hubble diagram of velocity (top) and value of H_0 (bottom) as a function of distance. Freedman et al. (2001), © 2001 The American Astronomical Society.*

The subscript zero hereby describes the present-day value of the constant. The constant H_0 is commonly called the Hubble constant and its value is about $H_0 = 70\,\mathrm{km\,s^{-1}\,Mpc^{-1}}$. Note that the Hubble constant is given in units of one over seconds. The reciprocal value of the H_0 thus defines a time, the so-called Hubble time. If the expansion of the universe is never accelerated, its age could be determined as

$$t_0 \le \frac{1}{H_0} = 1.4 \times 10^{10}\,\mathrm{a}. \tag{2.7}$$

The distance of a galaxy is often expressed by its redshift. Let λ be the wavelength sent out from the galaxy in question and λ_0 the wavelength received today. The redshift z can then be written as

$$1 + z = \frac{\lambda_0}{\lambda} = \frac{R_0}{R}. \tag{2.8}$$

Here, R is introduced as the so-called scale factor of the universe.

Since the universe consists of mass that interacts gravitationally with each other, we can define a deceleration parameter q_0 for the universe such that

$$q_0 \equiv -\left(\frac{\ddot{R}R}{\dot{R}^2}\right)_0 f = -\frac{\ddot{R}_0}{R_0 H_0^2}. \tag{2.9}$$
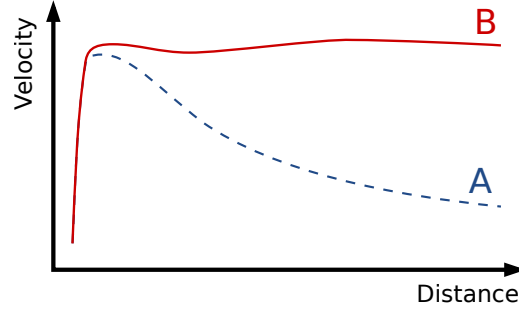
Figure 2.2.: *Galactic rotation: Case A shows the expected behavior, case B the observed one. Credit:* Wikipedia.

2.1.3. Density of Matter

By density one generally refers to the total energy density of all components (radiation, matter, and dark energy) divided by c^2. While radiation dominated in the early universe, matter or even dark energy dominates today. The total density of matter in the universe can be measured by determining the total mass of individual galaxies. An estimated density can thus be given as

$$2 \times 10^{-31} \, \mathrm{g\,cm^{-3}} \leq \rho_0 \leq 2 \times 10^{-30} \, \mathrm{g\,cm^{-3}}. \tag{2.10}$$

Dark matter In 1933, Fritz Zwicky noticed that galactic cluster do not rotate as expected. By constraining the observed mass in the cluster and observing its rotation, Zwicky noticed that some matter was missing. He called this dark matter. Figure 2.2 shows an example of the expected and observed rotation curves. From this and further observations we can derive that dark matter makes up around 85% of all matter in the universe. Only 15% of the matter in the universe consists of baryons, e.g., particles made up of quarks such as neutrons and protons.

2.1.4. Cosmic Microwave Background

In the Big Bang model, the universe started from a very hot and dense state. One expected remnant of this state is a relic radiation that in fact was detected in 1965 by Arno Penzias and Robert Wilson (Penzias & Wilson, 1965). The detection of this cosmic microwave background (CMB) is one of the pillars supporting the Big Bang model to describe the origin of the universe. The origin of the CMB will be discussed in further detail below.
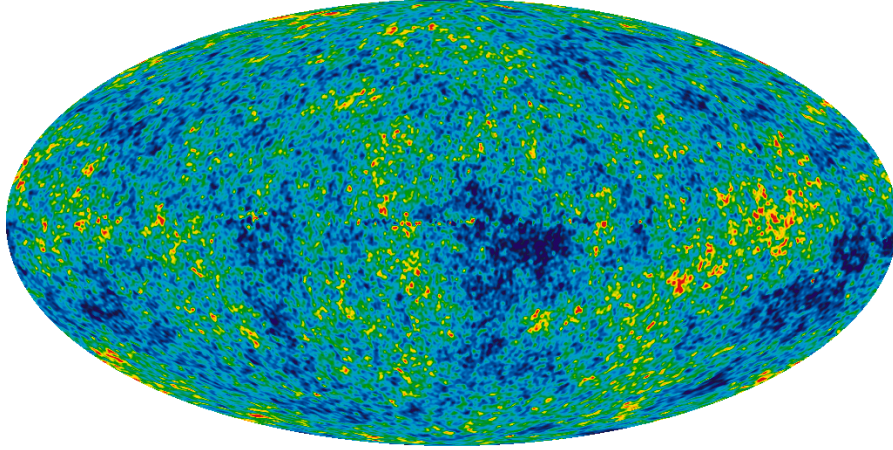
Figure 2.3.: *WMAP's image of the CMB. Shown is averaged data from nine years of measurements. Credit: NASA.*

The CMB is a thermal blackbody radiation with a measured temperature of 2.72548 ± 0.00057 K. The peak of this radiation is in the microwave range and cannot be observed from Earth. Space missions such as Wilkinson microwave anisotropy probe (WMAP) and Planck measured the CMB in detail. A map of the CMB is shown in Figure 2.3.
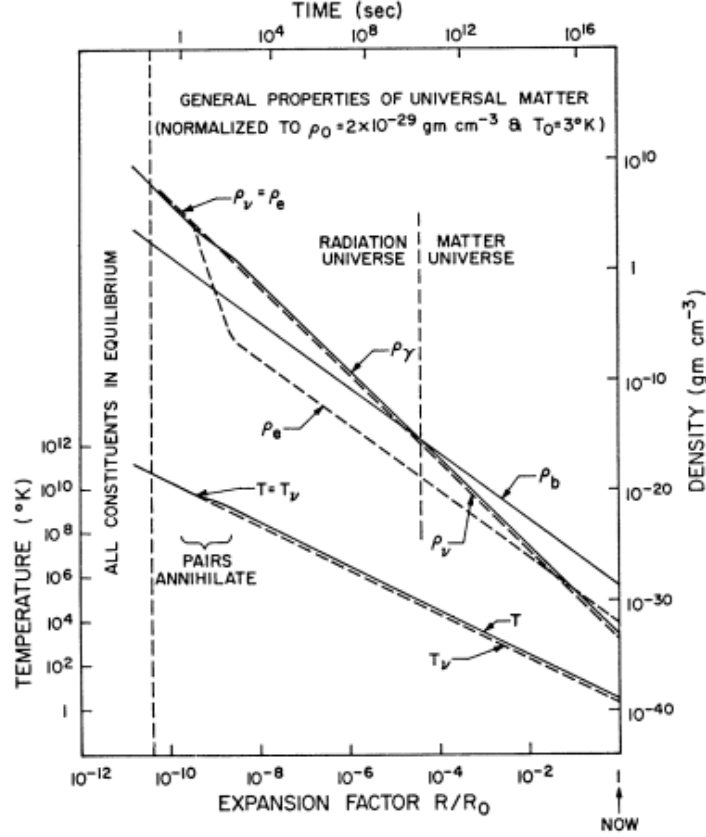
2.2. The Standard Model of Cosmology

The standard model of cosmology describes the origin of the universe and its evolution based on one singular event: the Big Bang. With the Big Bang, space, time, and matter came into existence and the universe developed from its hot, dense state to the cold and transparent state we see today.

2.2.1. Assumptions

The standard model of cosmology is based on several key assumptions. Here we focus on the ones that are of importance to understand BBN.

1. The cosmological principle is valid. This states that the spatial distribution of matter in the universe in homogeneous and isotropic.

2. The overall charge in the universe is zero.

3. The universe is made of matter and not of antimatter. This assumption in fact directly contradicts the cosmological principle (assumption 1) since it requires that there was an overabundance of baryons compared to antibaryons at the start of

Figure 2.4.: *The temperature and density evolution of the universe in the framework of the standard model of cosmology. Taken from Wagoner et al. (1967). © American Astronomical Society.*

the universe, making it thus inhomogeneous. This overabundance of matter is to this date not fully explained and remains under active investigation.

4. At temperature $T < 10^{11}$ K (approximately 10 ms after the Big Bang), all heavy particles were annihilated and the density of the universe is defined by photons, neutrinos (ν), electron and positrons ($e^{\pm}$), and the remaining baryons.

2.2.2. Temperature and Density Evolution

Figure 2.4 shows the temperature and density evolution of the universe in the framework of the standard model of cosmology (Wagoner et al., 1967). The horizontal axis show the expansion factor R/R_0 as defined in equation 2.8 on the bottom and the time since the Big Bang on the top. The vertical axes show the temperature (left) and the density (right). The standard model description starts at around 10 ms with all constituents in

23

equilibrium. Big Bang nucleosynthesis sets in at a temperature of around 10^9 K.

2.3. Big Bang Nucleosynthesis

2.3.1. The Proton-to-Neutron Ratio

In the beginning at a temperature of around 10^{11} K (see Figure 2.4), the protons and neutrons are in thermodynamic equilibrium. Statistical mechanics shows that the energy of such a system can be expressed using the Boltzmann distribution for the individual states. This can be used to express the ratio of the number of protons to the number of neutrons in equilibrium conditions as

$$\left(\frac{n_{\rm p}}{n_{\rm n}}\right)_{\rm eq} = \frac{\lambda_{\rm np}}{\lambda_{\rm pn}} = \exp\left(\frac{(m_{\rm n}-m_{\rm p})c^2}{kT}\right) = \exp\left(\frac{1.501}{T_{10}}\right). \tag{2.11}$$

Here, $\lambda_{\rm np}$ and $\lambda_{\rm pn}$ are the reaction rates to turn a neutron into proton and vice verse, respectively. For $T \to \infty$ protons and neutrons will have equal abundances. At lower temperatures however, protons will become more abundant.

We can rewrite equation (2.11) to express the mass fractions of neutrons in equilibrium as

$$X_{\rm n,eq} = \left(\frac{n_{\rm n}}{n_{\rm p}+n_{\rm n}}\right)_{\rm eq} = \frac{1}{(n_{\rm p}/n_{\rm n})_{\rm eq}+1} = \frac{\lambda_{\rm pn}}{\lambda_{\rm pn}+\lambda_{\rm np}}. \tag{2.12}$$

The nucleons react with each other via the weak force and the following reactions are possible:

$$n + \nu \longleftrightarrow p + e^- \tag{2.13}$$
$$n + e^+ \longleftrightarrow p + \bar{\nu} \tag{2.14}$$
$$n \longrightarrow p + e^- + \bar{\nu} \tag{2.15}$$

Reaction (2.15) is the free decay of neutrons and has a half-life of $610\,$s. This reaction can thus be neglected at the beginning since it is very long compared to all other reactions. The neutron mass fraction over time follows thus the differential equation

$$\frac{d}{dt}X_{\rm n}(t) = -\lambda_{\rm np}(t)X_{\rm n}(t) + \lambda_{\rm pn}(t)[1-X_{\rm n}(t)]. \tag{2.16}$$

With decreasing temperature the reaction rates $\lambda_{\rm np}$ and $\lambda_{\rm pn}$ go rapidly towards zero such that after around $10\,$s the proton to neutron ratio is frozen in place. Calculating reaction rate values, e.g., as in Peebles (1966b), the neutron mass fraction at freezeout (when the reaction rates $\lambda_{\rm np}$ and $\lambda_{\rm pn}$ go to zero) is

$$X_{\rm n,freeze} = 0.164. \tag{2.17}$$

From this time on, the only reaction taking place is free neutron decay, see reaction (2.15). Since the half-life of neutrons is fairly short, they must rapidly after the freezeout be captured as part of atomic nuclei in order to not decay away.

2.3.2. Nucleosynthesis of Deuterium

Deuterium has a mass of $m_D = 1875.612928\,\text{MeV}$, while a proton and neutron have masses of $m_p = 938.272088\,\text{MeV}$ and $m_n = 939.565421\,\text{MeV}$ (see info box below for an explanation of measurements in eV). Deuterium, an isotope of hydrogen (^2H), consists of one proton and one neutron. However, summing the mass of one proton and one neutron results in a mass that is $\Delta m = 2.22\,\text{MeV}$ larger than the mass of deuterium. This so-called mass defect defines the binding energy of deuterium and is the reason why energy is released when a proton and neutron are fused together. In chemistry this would be called an exothermic reaction. It can be written as

$$\text{p} + \text{n} \longrightarrow \text{D} + \gamma. \tag{2.18}$$

At the time when n_p/n_n is frozen, the temperature of the universe is still $T \approx 5 \times 10^9\,\text{K}$. Any deuterium that forms at this temperature is effectively destroyed right away again, since many photons have enough energy to dissociate the binding energy of $2.22\,\text{MeV}$. Figure 2.5 shows the spectral energy of a blackbody at this high temperature as a function of the frequency of the photons (bottom axis) and as function of their energy in MeV (top axis). The black, dashed line shows the deuterium binding energy. Note that both axes of the figure are logarithmic. Clearly, at $T_9 = 5$ many photons still have high enough energies. The universe thus first needs to cool down below $T_9 \approx 1$ before deuterium can effectively form.

The exact temperatures, as just described, do not only depend on the temperature but also on the abundance of photons. Furthermore, the temperature is directly related

Measurements in eV In nuclear physics, masses are often expressed in mega electronvolts or MeV, which is technically not a mass but an energy. The mass of the particle is related to its energy via Einstein's equation $m = E/c^2$. Thus, energy and mass are directly related with c, the speed of light, as a proportionality constant. Similarly we can write the momentum of a particle as $\vec{p} = E\vec{c}^{-1}$ and the temperature of a system as $T = Ek_B^{-1}$. Here, k_B is the Boltzmann constant. Since mass, momentum, and temperature are related to energy via constants, these quantities are often expressed as energies.
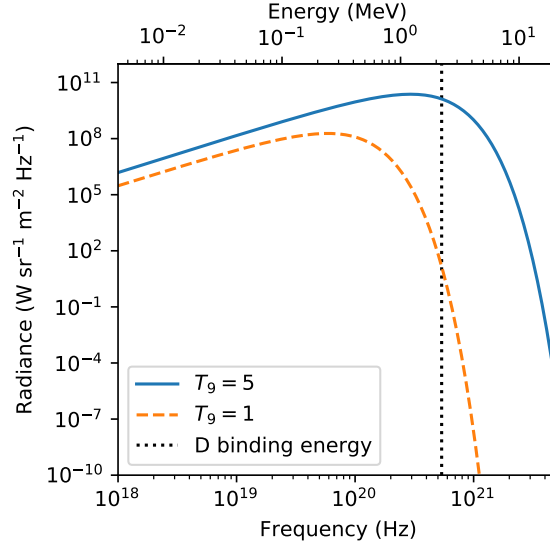
Figure 2.5.: *Spectral energy of black body radiation at the temperature when neutrons and protons are in equilibrium ($T_9 \approx 5$) and when deuterium fusion can start ($T_9 \approx 1$). Prior to this temperature, the photon energies are too high and destroy newly formed deuterium effectively.*

to the density of the universe. Figure 2.5 thus only gives a relative insight into the dissociation of deuterium. More detailed calculations can be found in the literature, e.g., in Wagoner et al. (1967).

The drop in temperature of the universe from when proton and neutron abundances are frozen until deuterium can effectively form without being destroyed takes about 220 s. During this time, the neutrons still undergo free decay. Using equation (1.2) we can calculate that by the time deuterium fusion becomes significant, another $\sim 20\%$ of the neutrons decay. This leaves behind a neutron fraction of

$$X_n = 0.128 \tag{2.19}$$

at the start of BBN.

2.3.3. Nucleosynthesis of Helium

Once deuterium has formed, more reactions can take place. Some of these reactions are:

$$D + D \longleftrightarrow {}^3\text{He} + n \tag{2.20}$$
$$T + p \longleftrightarrow {}^3\text{He} + n \tag{2.21}$$
$$T + D \longleftrightarrow {}^4\text{He} + n \tag{2.22}$$
$$p + D \longleftrightarrow {}^3\text{He} + \gamma \tag{2.23}$$
$$n + D \longleftrightarrow T + \gamma \tag{2.24}$$
$$p + T \longleftrightarrow {}^4\text{He} + \gamma \tag{2.25}$$
$$n + {}^3\text{He} \longleftrightarrow {}^4\text{He} + \gamma \tag{2.26}$$
$$D + D \longleftrightarrow {}^4\text{He} + \gamma \tag{2.27}$$

Here, T is a tritium nucleus, another isotope of hydrogen with two neutrons (^{3}H). The reaction rates for these individual paths can be calculated, however, let us first estimate the dominant product of big bang nucleosynthesis. For deuterium above we determined a binding energy of 2.22 MeV. Calculating the mass defect and thus the binding energy for ^{3}He and ^{4}He gives 6.70 MeV and 27.3 MeV, respectively. A better way to compare these binding energies is however to determine the binding energy per nucleon. For ^{3}He and ^{4}He these would be 2.23 MeV per nucleon and 6.81 MeV per nucleon. Thus, ^{4}He is much favored to being produced.

If we assume that all neutrons will be bound into ^{4}He, a fairly accurate assumption as we will see further down, we can now predict the mass fraction of helium (Y) in the universe. After free decay of neutrons, we are left with $X_\text{n} = 0.128$. Since ^{4}He is roughly four times heavier than hydrogen, we can estimate the mass fraction of ^{4}He as

$$Y = \frac{4n_\text{He}}{4n_\text{He} + n_\text{H}} = \frac{2n_\text{n}}{n_\text{p} + n_\text{n}} = \frac{2(n_\text{n}/n_\text{p})}{1 + (n_\text{n}/n_\text{p})} = 0.23. \tag{2.28}$$

This estimated value is in excellent agreement with the observed abundance of helium in the universe of about 1/4 and is thus another robust pillar for the Big Bang model.

2.3.4. Nucleosynthesis of heavier elements

The highest binding energy per nucleon is found in the isotope ^{62}Ni. However, several reasons contribute to the fact that BBN cannot synthesize nuclides heavier than ^{7}Li.

Figure 2.6 shows an excerpt of the chart of the nuclides from hydrogen to carbon. Black isotopes are stable. The dashed, red lines indicate mass numbers $A = 5$ and $A = 8$, at which no stable nuclides exist. Thus, reactions of two ^{4}He nuclei or a ^{4}He nucleus and a proton do not form stable nuclides, which prevents BBN from forming anything heavier than ^{7}Li.
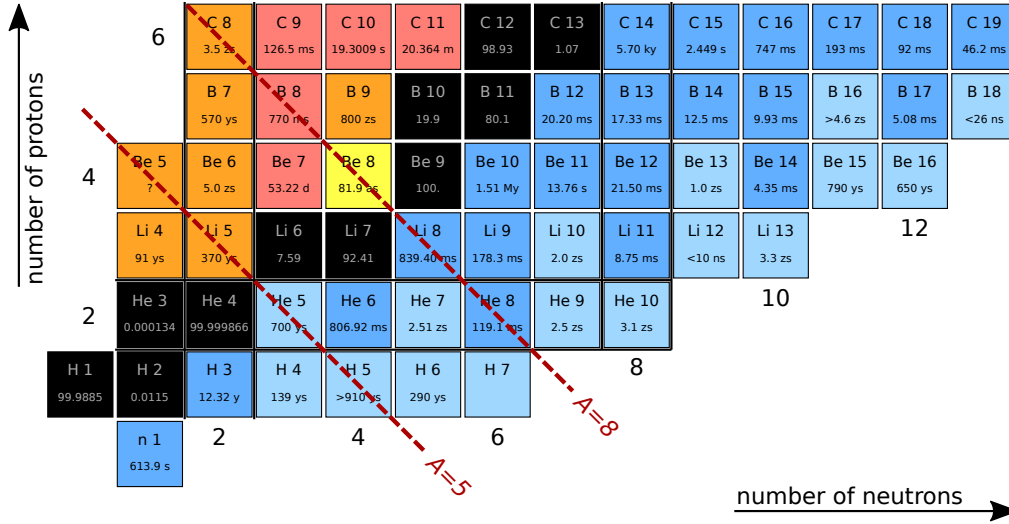
Figure 2.6.: *The low-mass section of the chart of the nuclides with red, dashed lines indicating $A = 5$ and $A = 8$. These are the two mass regions that do not have any stable nuclides, thus effectively halting heavier element production in BBN. Chart generated with a python tool by Krzysztof Miernik.*

While nucleosynthesis takes place, the universe continues expanding, thus the temperature further decreases. This significantly limits the time in which new nuclides can form. Below a temperature of $T_9 \approx 0.1$ BBN comes to a halt. This means that around 10-15 min after the Big Bang, all the hydrogen, helium, and other BBN products were formed.

Figure 2.7 shows the reaction network showing dominant reactions at work in BBN (after Nollett & Burles, 2000). As is common, we abbreviate the ^{4}He nucleus with the symbol α. Reactions are written in their abbreviated form, as is common in nuclear physics. For example ^{1}H(n,γ)^{2}H could also be written as ^{1}H + n $\longrightarrow$ ^{2}H + γ. Notably, there is no main reaction to produce ^{6}Li. Lithium-7 can be produced in two ways: directly from tritium by capturing a α particle (which is equivalent to ^{4}He capturing a tritium nucleus) or by production of ^{7}Be (from ^{3}He) and subsequent decay to ^{7}Li.

2.3.5. Observational Constraints

So far, we have roughly derived the production of hydrogen and ^{4}He expected to form during the Big Bang. We furthermore mentioned how D, ^{3}He, and ^{7}Li are produced. Our derivations were mainly based on the temperature and density evolution of the universe during BBN, two quantities that are coupled to each other. By observing the abundances of hydrogen, helium, and lithium in the universe and deriving the fractions of the species of interest that formed in the Big Bang, we can constrain the environment
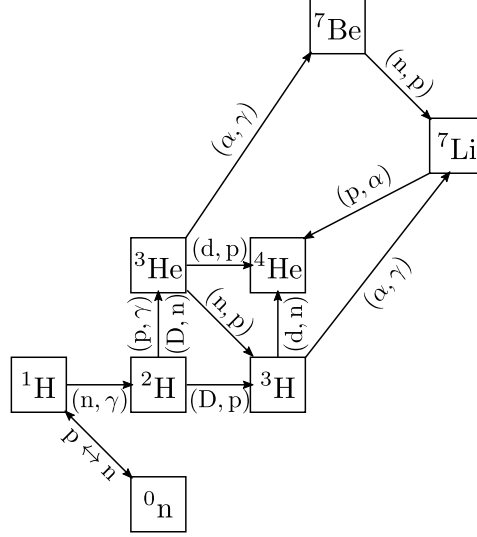
Figure 2.7.: *BBN reaction rate network for dominant reactions, after Nollett & Burles (2000).*

in which BBN took place.

Figure 2.8 shows the calculated abundances of D, ^{3}He, ^{4}He, and ^{7}Li when varying the present-day baryon density. The squares show the observed ratios, where available, and their uncertainties. The larger the baryon density in the universe, the larger is the baryon-to-photon ratio. As discussed before, this ratio and the temperature define when deuterium can form (see Figure 2.5). If the baryon-to-photon ratio goes up, fewer neutrons decay until they are captured and thus more ^{4}He nuclei are ultimately formed. The conversion of D to ^{4}He will also be more complete, thus less deuterium remains. The higher starting abundance of D and higher end abundance of ^{4}He also results in burning out ^{3}He more effectively, thus lowering its abundance with an increase in the baryon density. The curve in Figure 2.8 for ^{7}Li shows the competition of two reactions. At low baryon densities, ^{7}Li is mainly produced via ^{4}He + T $\longrightarrow$ ^{7}Li + ν. At increased baryon density, ^{7}Li however gets again efficiently destroyed by burning further. This destruction is compensated and overtaken at even higher baryon densities since ^{7}Be is produced more efficiently, which then immediately decays to ^{7}Li.

While difficult to observe, the abundance of BBN-produced hydrogen, helium, and lithium in the universe is a great way to determine crucial parameters of the Big Bang model. Similar insights can however also be gained by analyzing the CMB.
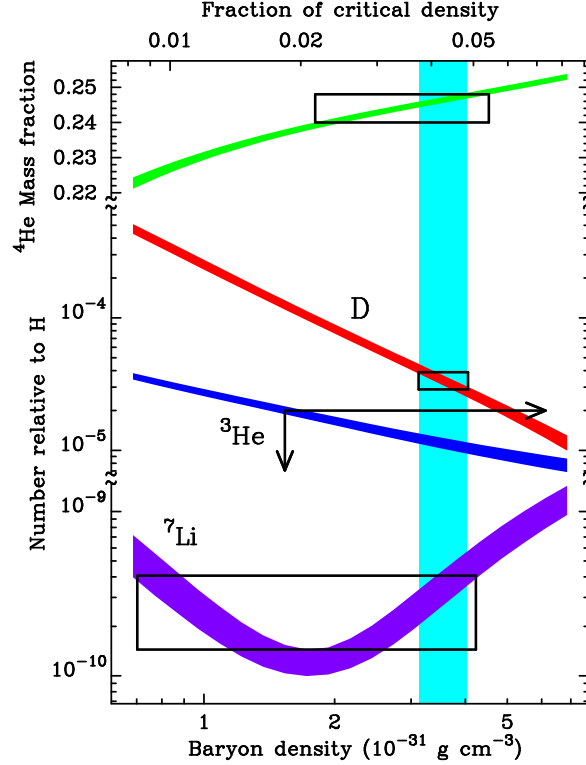
Figure 2.8.: *BBN predictions of the D, ^{3}He, ^{4}He, and ^{7}Li abundance as a function of the present-day baryon density (Tytler et al., 2000). From* `arXiv:astro-ph/0001318`.

2.4. Recombination

In Section 2.2.1 we laid out the assumptions of the standard model of cosmology, one of which is that the overall charge in the universe is zero. During BBN, the temperature too high to for electrons and nuclei to combine in order to produce a neutral gas. These components thus rather occur as a plasma. In order to create a neutral gas, the temperature has to sink to below 3000 K. At this temperature, the electrons combine with the atomic nuclei. Historically, this phase has been described as recombination, although the "re" part is slightly misleading since electrons and nuclei have never been combined previously.

During the plasma phase, i.e., prior to recombination, photons can scatter easily and the universe is thus opaque. After recombination the universe becomes transparent, and we transition into the matter dominated universe (see Figure 2.4). Since the Big Bang, roughly 4×10^5 a have elapsed at this point.

The transition from the radiation dominated to the matter dominated universe can still be seen today as the horizon of the visible universe. It has significantly cooled down and is today seen as the CMB. An image of is fluctuations is shown in Figure 2.3.

2.5. Reading

Since BBN took place fairly long ago at this point, it seems adequate to also look at the literature from a historic point of view. For the historical perspective one should read Alpher et al. (1948) and Peebles (1966a). Focus on comparing the two manuscripts: what are the differences between them and what are differences compared to what you have learned in class?

The present status of BBN was recently given by Cyburt et al. (2016). While this work contains fairly detailed methods on uncertainty calculations that are outside the scope of this lecture, the eager student might want to read sections III. Observations and V. The Lithium Problem in detail. You might also want to skim the introduction and the preliminaries.

For these readings it is important that you do not get hung up on details you do not understand, but rather try to follow the big picture. The following questions that can be discussed in class might help to focus on the big picture.

- What elements and isotopes are all formed in the Big Bang according to the work by Alpher et al. (1948)? What are the issues you see with this model, especially regarding it from the current state of knowledge?

- What nuclides were produced in the Big Bang according to Peebles (1966a) and how does this differ from the work by Alpher et al. (1948)?

- Note the neutron half-life that is used in Peebles (1966a). What is the issue here? This is also in detail discussed in the introduction by Cyburt et al. (2016).

- What importance does the nuclear reaction rate network have in Cyburt et al. (2016)? What reaction rates are to this day fairly uncertain?

- Discuss how the primordial abundance of H, D, ^{3}He, ^{4}He, and ^{7}Li can be derived from current observations. What are the problems?

- What is meant in Cyburt et al. (2016) by "regression to zero metallicity"?

3. Star Formation

In the last chapter we discussed the formation of the first elements in the Big Bang and derived that all the hydrogen and the vast majority of helium we see today in the universe formed in this event. In this chapter we will study how stars can form from hydrogen and helium gas and how they evolve throughout their lifetime. This topic is discussed generally for all stars, however, we will in the end focus on the very first and oldest star to form in the galaxy.

3.1. Molecular Cloud Collapse and Protostar Formation

To understand star formation, let us first discuss how molecular clouds collapse. Figure 3.1a shows a Hubble Space Telescope (HST) image of the famous horsehead nebula, a molecular cloud located in the constellation Orion. Molecular clouds are accumulations of gas and dust in the galaxy that prevent light from the stars behind it to come through. These structures thus look like clouds to the observer.

3.1.1. Jeans Criterium for Gravitational Collapse

For simplicity, let us assume a spherical, homogeneous sphere with a constant density ρ and temperature T. A schematic of such an idealized molecular cloud is shown in Figure 3.1b. The gravitational / potential that a given test mass m in the molecular cloud is in can be written as

$$E_{\text{pot}} = -\frac{GMm}{R}. \tag{3.1}$$

Here, R is the distance of the test mass from the center of the molecular cloud and M is the total mass of the cloud inside the radius R. Furthermore, G is the gravitational constant and is equal to $G = 6.674 \times 10^{11}\,\text{m}^3\,\text{kg}^{-1}\,\text{s}^{-2}$. Infinitely far away from the molecular cloud, the gravitational potential is by definition zero. Thus, it becomes negative the closer to the center the test mass gets.

Instead of a test mass, let us now assume that we want to determine the gravitational energy of a mass shell with thickness dr at distance r from the center of the molecular cloud. A schematic of this setup is shown in Figure 3.1b. Assuming that the cloud is at

(a) The horsehead nebula. Credit: NASA/ESA/Hubble Heritage Team.
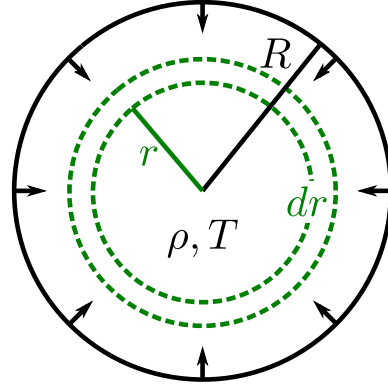
(b) A schematic representation of a molecular cloud collapsing.

Figure 3.1.: *Molecular clouds are the structures stars form from in the universe.*

a given temperature T and has a homogeneous density ρ, we can write the mass of the shell (m) and the mass of the cloud inside the shell (M) as

$$m = 4\pi\rho r^2 dr \tag{3.2}$$

$$M = \frac{4}{3}\pi\rho r^3. \tag{3.3}$$

We can now determine the total potential energy of the molecular cloud as

$$
\begin{aligned}
E_{\text{pot}} &= -\int_0^R \frac{G}{r}\left(\frac{4}{3}\pi\rho r^3\right)\left(4\pi\rho r^2\right) dr \\
&= -\frac{16}{3}\pi^2\rho^2 G \int_0^R r^4 dr \\
&= -\frac{16}{15}\pi^2\rho^2 G R^5 \\
&= -\frac{3}{5}G\frac{M^2}{R}.
\end{aligned}
\tag{3.4}
$$

In the last step we used the fact that the mass of the molecular cloud can be written as

$$M = \frac{4}{3}R^3\rho \tag{3.5}$$

to substitute it back into the equation.

During the collapse, gravitational energy is transformed into kinetic energy, which here is equal to a rise in temperature. The total kinetic energy of the system can be written as

$$E_{\text{kin}} = \frac{3}{2} N k T = \frac{3}{2} k T \frac{M}{\mu}, \tag{3.6}$$

where N is the number of molecules in the molecular cloud and μ their average mass, i.e., to first approximation the mass of H_2. For a cloud in hydrostatic equilibrium, i.e., a cloud that is neither expanding nor contracting, the virial theorem (which is derived in Appendix A) can be applied. This theorem states that the kinetic and potential / gravitational energy are related to each other as

$$2E_{\text{kin}} + E_{\text{pot}} = 0. \tag{3.7}$$

Assuming the molecular cloud is in equilibrium, we can plug equations (3.4) and (3.6) into (3.7) and solve for the mass.

$$3kT\frac{M}{\mu} - \frac{3}{5}G\frac{M^2}{R} = 0$$
$$\frac{GM}{5R} = \frac{kT}{\mu} \tag{3.8}$$
$$M = \frac{5RkT}{G\mu} \equiv M_J$$

Here, M_J is the so-called Jeans mass, named after Sir James Jeans who first described this derivation in 1904. It describes the mass $M = M_J$ for which the molecular cloud is in balance, i.e., the kinetic and gravitational energy compensate each other. The Jeans mass thus also describes the minimum mass for star formation; a molecular cloud with $M > M_J$ will collapse since the gravitational force dominates.
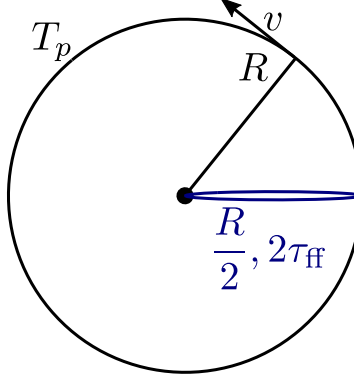
3.1.2. Free Fall Time

To determine how long gravitational collapse of a molecular cloud takes, we can estimate the free fall time. The gravitational force of the system and its radius are known. Using Newton's law $\vec{F} = m\vec{a}$, we can thus write the slightly unwieldy differential equation

$$-G\frac{Mm}{R^2} = m\ddot{R}, \tag{3.9}$$

where m is a test mass at the edge of the cloud. However, the free fall time τ_{ff} can also be derived more elegantly. Kepler's third law of planetary motion states that the cube of the semi-major axis of a planet divided by the square of its period is constant. This law in fact can directly be derived by comparing the gravitational and centrifugal force acting on a planet since these two forces, for a stable orbit, must compensate each

Figure 3.2.: *Schematic to derive the free fall time τ_{ff} using Kepler's third law of planetary motions. See text for details.*

other. Figure 3.2 shows a schematic of the here discussed scenario. The molecular cloud (black circle), if not collapsing, would have to rotate at a given velocity v such that the gravitational force F_g and the centrifugal force F_c compensate each other. For a test mass at the outermost edge of the cloud, the gravitational force of the whole cloud is equivalent as if we pictured the mass of the cloud to be concentrated in the center. Disregarding vector quantities, we can derive the velocity a stable cloud would move around the center with as

$$F_g = F_c$$
$$G\frac{Mm}{R^2} = \frac{mv^2}{R} \tag{3.10}$$
$$\Rightarrow v = \left(G\frac{M}{R}\right)^{1/2}.$$

k To determine the free fall scenario we can now halt the test particle in its motion, i.e., set $v = 0$. The "orbit" of the test particle would then look like a straight line into the gravitational center of the cloud. In Figure 3.2 this scenario is shown by drawing the line as a very skinny ellipse. The semi-major axis of this orbit would now be $R/2$ and the orbital period $2\tau_{ff}$.
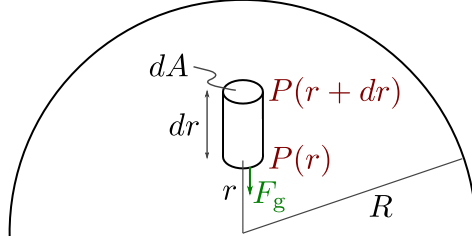
From Kepler's third law we know that the following statement must hold true.

$$\frac{R^3}{T_P^2} = \frac{\left(\frac{R}{2}\right)^3}{(2\tau_{ff})^2} \tag{3.11}$$

Here, T_P can be derived using the velocity as given in equation 3.10 and the length of the orbit $(2\pi R)$. This yields

$$T_p = 2\pi \left(\frac{R^3}{GM}\right)^{1/2}. \tag{3.12}$$

Figure 3.3.: *Schematic drawing to derive the hydrostatic equilibrium equation. See text for details.*

Plugging equation (3.12) into equation (3.11) and expressing the mass of the cloud using the density ρ as $M = \frac{4}{3}R^3\rho\pi$, we can finally derive the free fall time as

$$\tau_{\text{ff}} = \left(\frac{3\pi}{32G\rho}\right)^{1/2}. \tag{3.13}$$

3.1.3. Protostar Birth

Fortunately, the molecular cloud collapse does not take place adiabatically. Heat is effectively radiated from the cloud as infrared radiation (IR), thus preventing the Jeans mass (which is proportional to the temperature) from exceeding the molecular cloud mass and thus bringing the cloud into hydrostatic equilibrium (see Section 3.2). The main cooling mechanisms producing IR radiation are molecular collisions and dust. Colliding molecules transfer energy into vibrational states which, when they decay, emit IR. Dust on the other hand will heat up and radiate as a blackbody with an effective temperature of less than around $1000\,\text{K}$, thus mostly radiating in the IR. The molecular cloud is mostly transparent to IR and can thus effectively cool thanks to these processes.

Ultimately, the rising heat will start dissociating molecules and evaporating dust, thus the effective cooling mechanism stops. At this point the temperature in the center rises and the Jeans mass will be exceeded. The center of the collapsing cloud defines the protostar in hydrostatic equilibrium (see below).

3.2. Hydrostatic equilibrium

Once a molecular cloud has reached a high enough temperature such that its mass is equal to the Jeans mass, the system has entered the so-called hydrostatic equilibrium. Understanding this equilibrium is crucial in terms of understanding stellar phases during the end of their lives and during nucleosynthesis events. The whole life of a star is dominated by hydrostatic equilibrium.

Figure 3.3 shows a cylinder of length dr, face area dA, and density $\rho(r)$ at distance r from the center of the star. The gravitational force that acts on the cylinder can be written as

$$F_{\mathrm{g}} = -G\frac{M_r dm}{r^2}, \tag{3.14}$$

where M_r is the mass of the star that is inside radius r and $dm = \rho(r)drdA$ is the mass of the cylinder.

In addition, the cylinder is under pressure, i.e., the pressure $P(r + dr)$ from above it pushing it down and the pressure $P(r)$ from below it pushing it up. To force exerted by the pressure is

$$F_P = dPdA, \tag{3.15}$$

where $dP = P(r + dr) - P(r)$.

In order for the cylinder to be neutrally buoyant, i.e., to be in hydrostatic equilibrium, the gravitational force must exactly compensate the force exerted by the pressure. Setting equations (3.14) and (3.15) equal plus some simple algebra, we can derive the hydrostatic equilibrium condition as

$$\frac{dP}{dr} = -\rho(r)\frac{GM_r}{r^2}. \tag{3.16}$$

3.2.1. Central Pressure

Using equation (3.16), we can estimate the central pressure of a star by integrating over r. For this estimate, let us replace the density $\rho(r)$ with the mean density inside the star. This mean density can be expressed as

$$\bar{\rho} = \frac{M}{\frac{4}{3}\pi R^3}. \tag{3.17}$$

We can furthermore write M_r as a function of the distance r from the center of the star. Remember that M_r simply represents the mass of the star inside of radius r, thus

$$M_r = M(r) = \frac{4}{3}\pi r^3 \bar{\rho}. \tag{3.18}$$

Plugging these two quantities into equation (3.16) and integrating over r, the central pressure P_c can be estimated as

$$P_c = \frac{3}{8\pi}\frac{GM^2}{R^4}. \tag{3.19}$$

We assumed here that the pressure at the surface of the star is zero, which is surely true when compared to the central pressure. In the case of the Sun, using equation (3.19) we can calculate a central pressure of $P_{c,\odot} \approx 10^{14}$ Pa.

Note that the presented estimate of the central pressure of a star necessarily represents a lower limit. The reason for this is that we assumed a constant density throughout the star, which surely is not correct. The density will be significantly higher in the center of the star compared to the outer parts. This always increases the pressure compared to our estimate. To visualize why, imagine all the mass of the star was concentration within $R/2$. Integrating the pressure over the whole star using our estimate above would result in the same central pressure. However, from our visualization we know that the central pressure is concentrated in the inner half, thus integration of r only needs to be done up to $R/2$ to determine the "real" central pressure. This value will necessarily be higher than what we estimated in equation (3.19).

For the Sun, $\rho(r)$ needs to be modeled in order to exactly determine the actual pressure. Such models yield a central pressure for the Sun of 2.5×10^{16} Pa, which is two orders of magnitude higher than our lower limit estimate.

3.2.2. Central Temperature

From the estimated central pressure, we can estimate the central temperature of a star assuming that the equation of state of an ideal gas holds in this scenario. This equation takes the form

$$pV = Nk_BT, \tag{3.20}$$

where p is the pressure, V the volume, N the number of particles, k_B Boltzmann's constant, and T the temperature. The number of particles that are in the gas can be expressed as $N = M/\mu$, where μ is the mean molecular weight of all particles. For a gas made of neutral hydrogen, the mean molecular mass per particle would be equal to the molecular mass of hydrogen μ_H. However, we know that the temperature within the Sun is so high that the hydrogen gas is fully ionized. Thus, we have twice as many particles (protons and electrons) to consider. Since electrons have significantly less mass than protons, the mean molecular mass of the gas inside a star can be estimated as $\mu = \mu_H/2$. Using equation (3.19), the central temperature of a star can now be written as

$$T_c = \frac{P_c\mu}{\bar{\rho}k_B}. \tag{3.21}$$

Here, we replaced N with M/μ, which results in V/M in this equation. This is of course equal to the reciprocal of the mean density ρ.

For the Sun, using the above determined pressure, we can estimate a temperature in the center of $T_{c,\odot} \approx 10^7$ K. Considering all the approximation that we made up to here, this number agrees strikingly well with the central temperature of the Sun.

3.2.3. Sustaining a Star via Gravity

Knowing the luminosity L of a star, e.g., the luminosity of the Sun, which is $L_\odot = 3.828 \times 10^{26}\,\text{W}$, we can calculate how long the star would live if it its energy would solely originate from gravitational collapse. The total gravitational energy available in the system is already given in equation (3.4). Since the luminosity is simply energy per time, the total amount of time that a star's luminosity could be sustained by gravitational infall is

$$t = \frac{E_\text{g}}{L} = \frac{GM^2}{RL} \equiv t_\text{KH}. \qquad (3.22)$$

This time is also known as the Kelvin-Helmoltz time (t_KH).

For the Sun we can calculate that gravity alone would be able to sustain the current luminosity for a total of $t_\text{KH} = 3 \times 10^7\,\text{a}$. This time is more than two orders of magnitude too short. Looking at the Earth's fossil record, clear evidence has been found for live on Earth as far back as $3.5\,\text{Ga}$ (Schopf et al., 2007). Dating meteorites furthermore yields a Solar System age of $4.567\,\text{Ga}$. Thus, the Sun must be at least be 100 times older than indicated by the Kelvin-Helmholtz time and another energy source is required to hold up the hydrostatic equilibrium.

3.2.4. Nuclear Reactions

We estimated the temperature at the center of the Sun to be $T_c \approx 10^7\,\text{K}$, which is high enough to efficiently convert hydrogen to helium. Nuclear reactions are in fact the reason that stars can sustain the hydrostatic equilibrium. In Section 2.3.3 we established that converting four hydrogen atoms into one helium atom releases $\Delta E = 28.3\,\text{MeV}$ of energy. If all the hydrogen mass (M_H) of a star is available as fuel to sustain the hydrostatic equilibrium, the star's lifetime could be calculated as

$$t_\text{nuc} = \frac{M_\text{H} N_A \Delta E}{4\,m_\text{H} L}. \qquad (3.23)$$

Here, N_A is Avogadro's constant and $m_\text{H} = 1.008\,\text{g}\,\text{mol}^{-1}$ the molecular mass of hydrogen.

For the Sun, considering that hydrogen makes up $\sim 75\%$ of its mass, we can calculate $t_\text{nuc} \approx 10^{11}\,\text{a}$. However, not all the hydrogen is available as fuel since the Sun is not fully convective. Only around 10% of the hydrogen mass are accessible by the core and can thus be transformed to helium to produce energy. This puts the Sun's life while sustaining hydrostatic equilibrium via hydrogen burning at about $10\,\text{Ga}$, which means we have about $5\,\text{Ga}$ left.

3.2.5. The Death of a Star

When stars run out of fuel in the center, nuclear reactions can no longer be sustained and thus the radiation pressure falls away. The star is thus no longer in hydrostatic equilibrium since $dP/dr = 0$ in equation (3.16). Therefore, the system will start collapsing again due to gravitation. The temperature in the center of the star will rise further until the next burning stage can start, i.e., helium burning in the triple α process producing ^{12}C. These reactions produce again radiation pressure, thus reestablishing the hydrostatic equilibrium. How many burning stages can be accessed by the star depends on the star's initial mass and will be discussed later.

Stellar evolution The evolution of stars is generally modeled using elaborate stellar evolution codes. Many different codes exist, however, one open-source stellar evolution code has recently be widely adopted. The Modules for Experiments in Stellar Astrophysics (MESA) code, developed by Bill Paxton at UCSB, has enabled many new research group to work on stellar evolution and its consequences. In fact, anybody can run and install MESA, instructions can be found on the MESA website. Note that while MESA is simple to use, users still must have some basic understanding of stellar evolution. The garbage in, garbage out concept applies to stellar evolution as well.

3.3. The Initial Mass Function

Star formation can only take place if a molecular cloud exceeds the Jeans mass. The likelihood of star formation in a given location of the galaxy depends on the density of material in that specific place. Depending on the total mass of the molecular cloud, stars of different masses can form. The so-called initial mass function (IMF) describes the number distribution of stars with different masses between $0.1\,M_\odot$ and $100\,M_\odot$ and has been derived from observations.

Figure 3.4 shows the IMF derived by three different researchers. The first IMF was published by Salpeter (1955). More detailed observations led to revisions of the IMF by Kroupa (2001) and Chabrier (2003). For stars heavier than $1\,M_\odot$, all IMFs agree with each other. At low masses, however, the IMF by Salpeter (1955) significantly overestimates the abundance of stars compared to the predictions by Kroupa (2001) and Chabrier (2003). Today, the latter two IMFs are generally used for GCE models.
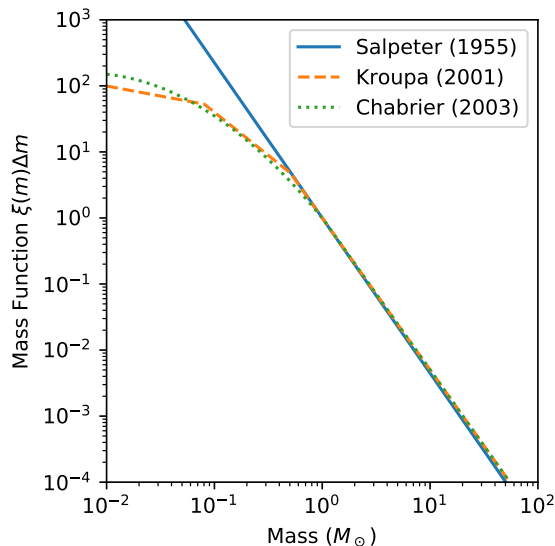
Figure 3.4.: *Comparison of* IMFs *by* Salpeter (1955), Kroupa (2001), *and* Chabrier (2003) *normalized to* $m = 1\,M_\odot$.

3.4. The First Stars

We have seen above that temperature and cooling play an essential role in star formation. The temperature of a molecular cloud is proportional to the Jeans mass, see equation (3.8). This leads to two issues: (1) The universe at the beginning was hotter, thus more mass is required for a molecular cloud to undergo gravitational collapse. (2) The main cooling processes of molecular clouds is to radiate heat away to not fall too early into hydrostatic equilibrium. This requires molecules and dust to be present. In the early universe the metallicity was however practically zero, thus this cooling process, except the dissociation of H_2 molecules, cannot take place. As a result only very massive, metal-free stars are expected to form in the beginning.

These predicted, very massive stars with very low metallicity are called population III stars. Metal poor stars with $10^{-4}\,Z_\odot < Z < 10^{-5}\,Z_\odot$, which can mostly be found in old globular clusters, are called population II stars. All more metal-rich stars, mostly found in the galactic disk, are population I stars, e.g., the Sun.

Massive stars, as we will see in detail later on, have a much shorter lifespan than low-mass stars and will thus quickly enrich the early universe with freshly nucleosynthesized products, i.e., metals. Thus, second and later generation will start off with some metallicity. Possible nuclear reactions thus change and get more diverse. To study these earliest stars and nuclosynthesis events, spectroscopic observations of ultra metal-poor stars are an important part.

3.5. Reading

For the curious reader, Anna Frebel wrote an excellent book titled "Searching for the Oldest Stars" (Frebel, 2015). The book is available via the Brandeis Library online.

For the discussion section we will focus on astronomical observations of Reticulum II, an ultrafaint dwarf galaxy that orbits the Milky Way. Please read Croswell (2021), a news feature article in the proceedings of the national academy of sciences. This article should give you a very brief and interesting overview of the field of the first stars, r-process nuclei, and why they are important for understanding element formation in the universe. Furthermore, this brief article is written as a summary of recent events and discoveries. Second, please read the paper by Ji et al. (2016) on the original observations of r-process enhanced stars in Reticulum II. This is the main article that we will discuss in class. The following bullet points should serve as guidance on reading these two manuscripts.

- What are r-process nuclides and why are they important in this context?

- What are ultrafaint dwarf galaxies? Why are they so interesting when studying the oldest stars? What population of stars do these galaxies contain? What is special about Reticulum II?

- Why were neutron star mergers thought to be the main contributor to r-process nuclei today, but not in the early universe? Has our thinking changed due to the work by Ji et al. (2016)? Has our thinking since then changed again?

- What is the difference between neutron-capture elements and non-neutron-capture elements? Why is this important in this context?

- Why do Ji et al. (2016) argue that all r-process elements in Reticulum II were made by one single event?

- What is the neutron star merger to supernova (SN) rate ratio in the Milky Way? What factor do you think play into the determination of the rates?

- What alternative scenarios could explain the observations of Ji et al. (2016) aside from neutron star mergers?

Bibliography

Allende Prieto, C. 2016, Living Reviews in Solar Physics, 13, 1 (40pp), doi: 10.1007/s41116-016-0001-6

Alpher, R. A., Bethe, H., & Gamow, G. 1948, Physical Review, 73, 803, doi: 10.1103/PhysRev.73.803

Asplund, M., Grevesse, N., Sauval, A. J., & Scott, P. 2009, Annual Review of Astronomy and Astrophysics, 47, 481, doi: 10.1146/annurev.astro.46.060407.145222

Bensby, T., Feltzing, S., & Oey, M. S. 2014, Astronomy & Astrophysics, 562, A71, doi: 10.1051/0004-6361/201322631

Chabrier, G. 2003, The Astrophysical Journal Letters, 586, L133, doi: 10.1086/374879

Croswell, K. 2021, Proceedings of the National Academy of Sciences, 118, doi: 10.1073/pnas.2026110118

Cyburt, R. H., Fields, B. D., Olive, K. A., & Yeh, T.-H. 2016, Reviews of Modern Physics, 88, 015004, doi: 10.1103/RevModPhys.88.015004

Frebel, A. 2015, Searching for the Oldest Stars: Ancient Relics from the Early Universe (Princeton University Press), doi: 10.2307/j.ctvc77mxp

Freedman, W. L., Madore, B. F., Gibson, B. K., et al. 2001, The Astrophysical Journal, 553, 47, doi: 10.1086/320638

Heber, V. S., Wieler, R., Baur, H., et al. 2009, Geochimica et Cosmochimica Acta, 73, 7414, doi: 10.1016/j.gca.2009.09.013

Ji, A. P., Frebel, A., Chiti, A., & Simon, J. D. 2016, Nature, 531, 610, doi: 10.1038/nature17425

Kroupa, P. 2001, Montly Notices of the Royal Astronomical Society, 322, 231, doi: 10.1046/j.1365-8711.2001.04022.x

Lodders, K. 2020, Solar Elemental Abundances, Oxford University Press, doi: 10.1093/acrefore/9780190647926.013.145

Bibliography

Lodders, K., Palme, H., & Gail, H. P. 2009, Landolt Börnstein, 4B, 712, doi: 10.1007/978-3-540-88055-4_34

Marty, B., Chaussidon, M., Wiens, R. C., Jurewicz, A. J. G., & Burnett, D. S. 2011, Science, 332, 1533, doi: 10.1126/science.1204656

McKeegan, K. D., Kallio, A. P. A., Heber, V. S., et al. 2011, Science, 332, 1528, doi: 10.1126/science.1204636

Nollett, K. M., & Burles, S. 2000, Physical Review D, 61, 123505, doi: 10.1103/PhysRevD.61.123505

Peebles, P. J. 1966a, Physical Review Letters, 16, 410, doi: 10.1103/PhysRevLett.16.410

Peebles, P. J. E. 1966b, The Astrophysical Journal, 146, 542, doi: 10.1086/148918

Penzias, A. A., & Wilson, R. W. 1965, The Astrophysical Journal, 142, 419, doi: 10.1086/148307

Salpeter, E. E. 1955, The Astrophysical Journal, 121, 161, doi: 10.1086/145971

Schopf, J. W., Kudryavtsev, A. B., Czaja, A. D., & Tripathi, A. B. 2007, Precambrian Research, 158, 141, doi: 10.1016/j.precamres.2007.04.009

Tytler, D., O'Meara, J. M., Suzuki, N., & Lubin, D. 2000, Physica Scripta, T85, 12, doi: 10.1238/physica.topical.085a00012

Wagoner, R. V., Fowler, W. A., & Hoyle, F. 1967, The Astrophysical Journal, 148, 3, doi: 10.1086/149126

Appendices

A. Deriving the Virial Theorem

We can use the hydrostatic equilibrium equation (3.16) to derive the virial theorem that has been used extensively in Chapter 3. To start we can multiply the hydrostatic equilibrium equation (3.16) on both sites by $4\pi r^3 dr$ and integrate over r. Writing this out gives us

$$\int_0^R 4\pi r^3 \frac{dP}{dr} dr = -\int_0^R \rho G \frac{M(r)}{r^2} 4\pi r^3 dr. \tag{A.1}$$

Let us first discuss the right-hand side of the equation. Minor algebra of this side allows us to rewrite it since we know that $4\pi r^2 \rho dr$ is equal to the mass of a mass shell in the star with thickness dr at distance r from the center. We can thus write this whole part as dM. We then have to integrate over the mass instead of the radius. The right-hand side now looks like

$$-\int_0^R \left(\frac{GM(r)}{r} \right) 4\pi r^2 \rho dr = -\int_0^M \frac{GM(r)}{r} dM. \tag{A.2}$$

This part is of course equal to the gravitational or potential energy E_{pot}, see equation (3.1).

To evaluate the left-hand side of equation (A.1) we can use integration by parts for the integration over dr. Integration by parts states that

$$\int_a^b u(x)v'(x)dx = u(x)v(x)|_a^b - \int_a^b u'(x)v(x)dx. \tag{A.3}$$

We can set $u = 4\pi r^3$ and $v = P$ and write

$$\int_0^R 4\pi r^3 \frac{dP}{dr} dr = 4\pi Pr^3 |_0^R - \int_0^R 12\pi Pr^2 dr$$
$$= -3 \int_0^R 4\pi Pr^2 dr. \tag{A.4}$$

The first term $4\pi Pr^3 |_0^R$ is zero because at the inner limit $r = 0$ we know that $r(0) = 0$ and at the upper limit $r = R$ we can assume that $P(R) = 0$. Using the ideal gas equation

$$PV = Nk_B T \tag{A.5}$$

46

and the kinetic energy of an ideal gas, which is given as

$$E_{\text{kin}} = \frac{3}{2}Nk_BT, \tag{A.6}$$

we can write the pressure P as

$$P = \frac{2}{3}\frac{E_{\text{kin}}}{V}. \tag{A.7}$$

Plugging this expression for the pressure into equation (A.4), we can write for the left-hand side of equation A.1

$$E_{\text{kin}}\frac{1}{V}\int_0^R 4\pi r^2 dr. \tag{A.8}$$

For a sphere, $\int_0^R 4\pi r^2 dr$ is of course nothing else than its volume, V thus crosses out, and we have determined that the left-hand side of equation (A.1) is equal to $-2E_{\text{kin}}$. Thus, we have derived the virial theorem, which states that

$$-2E_{\text{kin}} = E_{\text{pot}}. \tag{A.9}$$